

RETROSPECTIVE REPRODUCIBILITY ANALYSIS OF STANDARD MRI PARAMETERS ACROSS THREE PRE-CLINICAL MOUSE TUMOUR XENOGRAFT MODELS

Firas Moosvi¹, Jennifer H.E. Baker^{2,3}, and Stefan A. Reinsberg¹

¹Physics and Astronomy, University of British Columbia, Vancouver, BC, Canada, ²BC Cancer Research Institute, Vancouver, BC, Canada, ³Physics and Astronomy, University of British Columbia, BC, Canada

Introduction

Target Audience: This work will be of use to mouse pre-clinical cancer researchers interested in the reproducibility of standard MRI measurements, particularly T_1 , $IAUC_{60}$, $IAUGC_{60}$, k^{trans} .

Purpose: This is a retrospective analysis of control animals imaged as part of other studies as a baseline for cross-site comparisons and in the design of future studies to estimate statistical power and expected effect size based on biological variability.

Methods

Animals: A total of 42 tumour bearing NOD/SCID mice were analyzed for this reproducibility study. Mice were implanted with one of three human tumour xenografts: BT474 (breast ductal carcinoma, $n=15$), MDA-361 (breast adeno carcinoma, $n=17$), or HT29 ($n=10$ colorectal carcinoma). The MDA-361, HT29, and 10 of the BT474 tumours were implanted subcutaneously in the dorsal region of a mouse, while the remaining 5 tumours were implanted orthotopically in the mammary fat pad. Tumours were imaged when they reached approximately 300mm^3 .

MRI: Imaging was performed using a 7T scanner (Bruker Biospec 70/30, Germany) with a volume coil transmit and a custom built surface receive coil. T_1 maps were acquired using a standard 2D multi-slice FLASH-based Look-Locker sequence. A subset of animals ($n=7$ animals, subcutaneous BT474 tumours) were imaged using a DCE-MRI 2D spoiled gradient echo sequence at a temporal resolution of 2.2 – 4s following an ~ 0.2 mL power injected bolus of Gd-DTPA-BMA (Omniscan, GE Healthcare; Milwaukee, WI) diluted to 0.05 mM/mL. Typical spatial resolution was 0.3mm x 0.3mm in-plane and 1-1.5mm through-plane with 6-8 slices acquired for each tumour.

Histology: Animals were euthanized following the last imaging session and tumours were immediately excised and frozen. Serial step cryosections 10 μm thick were obtained at 0.5 mm intervals and those corresponding to MRI slices were identified [1]. In all cases, sections were stained and imaged with CD31 (endothelium to identify blood vessels), Hoechst 33342 (nuclear dye to reflect cell density), and intravenously injected carbocyanine labeling of perfused vessels; a few tumours were also stained for TUNEL to mark apoptosis. Sections were imaged using a robotic microscope and camera to obtain tiled images of whole tumour sections [1].

Analysis: T_1 maps were obtained from the Look-Locker sequence by fitting the T_1 recovery equation to the complex data in a flip-angle independent fashion, as described by Chuang et al [2]. $IAUC_{60}$ was calculated using the normalized (baseline pre-Gd) signal intensity curves using Simpson's integration method and the $IAUGC_{60}$ was obtained using the concentration curve calculated using the baseline T_1 and the signal intensity at each time point. DCE-MRI data was analyzed by applying the extended Tofts model to the data and obtaining k^{trans} , v_e and v_p (data not shown in abstract). Regions of interest were manually drawn by a single observer in all cases.

Results and Discussion

General: Tumour size is often a confounding factor in pre-clinical cancer studies as tumour growth can vastly overshadow interventions. ROIs were used to estimate the tumour volume, $340 \pm 25 \text{ mm}^3$ (\pm std. error, $n=42$), indicating that observed parameter differences are unrelated to tumour size.

Result 1: Baseline T_1 depends on the tumour model. Voxels within each tumour were gathered and the distribution of the T_1 values is shown in Fig 1. as a normalized histogram. Unlike literature reported baseline T_1 values in normal tissues such as the brain, the variability in baseline T_1 in tumours is large (stdev: 415-550 ms) strongly suggesting the presence of heterogenous compartments within the tumour which have been confirmed histologically [1].

Result 2: Correlation of $IAUC_{60}$, $IAUGC_{60}$. There is a high correlation between $IAUC_{60}$ and $IAUGC_{60}$ ($r = 0.81$) indicating the model-free approach ($IAUC_{60}$) to analysing DCE-MRI data is sufficient in some cases. While the relationship between $IAUGC_{60}$ and pharmacokinetic parameters such as k^{trans} , v_e and v_p have been explored in great detail [3], the relationship between $IAUC_{60}$ and $IAUGC_{60}$ is unclear. Here we report that $IAUC_{60}$ is a suitable surrogate for $IAUGC_{60}$, particularly when considering $\Delta IAUC_{60}$ calculated before and after an intervention.

Conclusions: Implications of this study are two fold: 1) care must be taken when choosing pre-clinical models as the intra-tumour microenvironments tend to vary substantially and 2) when normalized, $IAUC_{60}$ is an appropriate surrogate for $IAUGC_{60}$ in DCE-MRI studies.

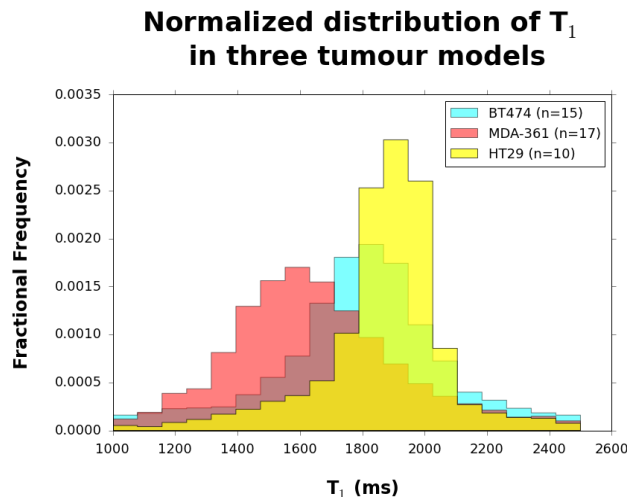


Fig. 1 - Voxel-wise distribution of T_1 values for three tumour cell lines across 42 animals, BT474 (aqua), MDA-361 (red) and HT29 (yellow) indicate that distinct tumour microenvironments contribute to a large range of T_1 values at baseline.

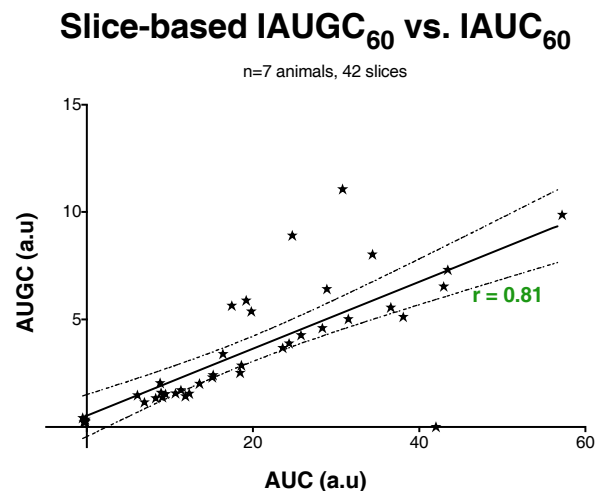


Fig. 2 - Slice-wise correlation plot of $IAUC_{60}$ and $IAUGC_{60}$ of T_1 7 BT474 tumours with each point representing a tumour slice average ($r = 0.81$, Spearman coefficient). Solid line is a best fit line and dotted lines indicate the 95% confidence interval.

References

- [1] Bains, L.J., Baker, J.H.E. et al. (2009). *International journal of radiation oncology, biology, physics*, 74(3), 957–965.
 [2] Chuang, KH et al (2006). *MRM* 55, 604-611, [3] Walker-Samuel S. et al. (2006). *Physics in Medicine and Biology* 51, 3593-3602